50th AIAA/ASME/ASCE/AHS/ASC Structures, Structural Dynamics, and Materials Conference
17th
4 - 7 May 2009, Palm Springs, California

AIAA 2009-2535

Fluid-Structure Transient Gust Sensitivity using Least-Squares Continuous Sensitivity Analysis

Douglas P. Wickert [1]
Air Force Institute of Technology, Wright-Patterson AFB, OH, 45433, USA

Robert A. Canfield [2]
Virginia Tech, Blacksburg, VA, 24061, USA

J. N. Reddy [3]
Texas A&M University, College Station, Texas 77843-3123, USA

A least-squares continuous sensitivity analysis method is developed for fluid-structure interaction transient gust response problems to support computationally efficient analysis and optimization of aeroelastic design problems. In continuous sensitivity methods, one computes design or shape parameter gradients from the continuous system of partial differential equations instead of the discretized system. The continuous sensitivity equations are a linear boundary-value problem which render computationally efficient design parameter gradients without needing to derive and code the problematic mesh sensitivities of discrete sensitivity methods. The coupled fluid-structure physics and continuous sensitivity system equations for a representative nonlinear gust response problem are posed in first-order form. The boundary conditions for the sensitivity system are derived from a least-squares formulation of the underlying fluid-structure problem. The continuous sensitivity boundary value problem is then solved using a high-order polynomial least-squares finite element model. An important distinction is made between local and total derivatives at material points of the structure and a method for converting the local sensitivities to material derivatives is developed. Continuous sensitivity results for both the local and total material derivatives are presented and compared to gradients obtained by finite-difference methods.

I. Introduction

Ongoing research efforts are seeking new methods for effective and computationally efficient analysis to support large-scale design optimization of elastic aircraft structures. One aspect of these efforts are high-fidelity, nonlinear, aeroelastic models suitable for aircraft gust response [1]. Another aspect of the research efforts involves creating effective surrogate models for efficient large-scale optimization [2]. Aeroelasticity is a challenging science, dealing with the interaction of two very different domains governed by disparate physics. Nonlinear aspects of both the fluid and structural domains can make accurate calculations of the interaction problematic, not the least due to the substantial computational expenses involved. Since optimization and inverse design methods typically require

The views expressed in this paper are those of the author and do not reflect the official policy or position of the United States Air Force, Department of Defense, or the United States Government.

[1] PhD Candidate, Department of Aeronautical and Astronautical Engineering, 2950 Hobson Way, Wright-Patterson AFB, OH 45433-7765, AIAA Member.

[2] Professor, Department of Aerospace and Ocean Engineering, 214 Randolph Hall, Blacksburg VA, 24061, AIAA Associate Fellow.

[3] Distinguished Professor, Department of Mechanical Engineering;jnreddy@.tamu.edu. AIAA Fellow.

some measure of the change of an objective function or performance parameter to variations in design parameters, optimization of aeroelastic problems, which are themselves computationally intensive, challenging, and expensive to solve, can be outright formidable. Thus, this subject represents a prime frontier for basic research

Design sensitivity methods can be grouped into numerical approximate methods (*e.g.* finite difference) and analytic/semi-analytic methods, Figure 1. Analytic and semi-analytic methods can be further classified as either discrete or continuous, the difference depending on the order of the discretization and differentiation steps [3, 4]. The most common approach is to discretize the system first and calculate sensitivities by either direct or adjoint methods. For shape sensitivity problems, the boundary and domain of the problem vary with the design parameters and the mesh sensitivity must also be calculated in the discrete approach. In the continuous sensitivity method, also known as variational shape design [3], the continuum sensitivity method [5], and the variational sensitivity method [6], the design parameter gradients are calculated by solving the continuous sensitivity equations (CSE), typically a system of partial differential equations [7]. Since the CSE system is posed as a continuous system, it can efficiently produce shape parameter gradients without calculating the mesh sensitivity (which often amounts to the expensive task of inverting a large mesh Jacobian). Further, the sensitivity system is always a linear system of equations, even when the original system is nonlinear.

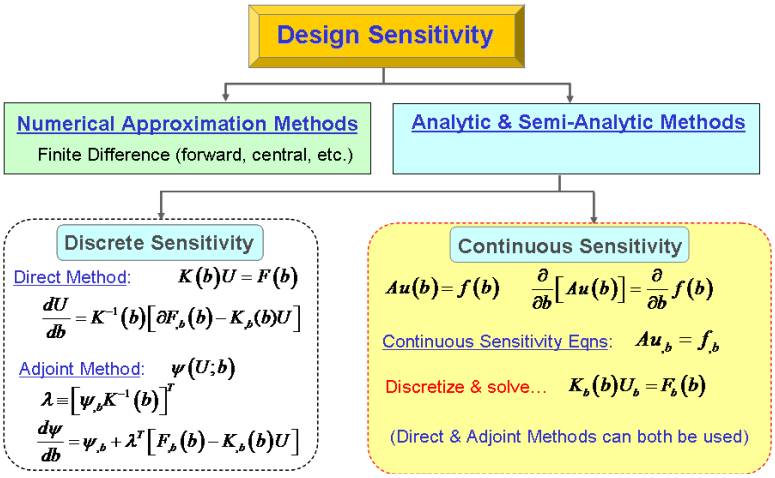

Figure 1: Classification and methods of design sensitivity analysis

Continuous sensitivity methods were first introduced for structural problems [5, 8], but few applications to structural problems appear in the literature. The landmark Borggaard and Burns paper [9] introduced the CSE nomenclature in a fluid setting and several fluid flow optimization applications followed [7, 10-12]. Although there now exists an extensive body of literature describing and documenting the application of continuous sensitivity methods to fluid dynamics problems, the applications to non-fluid problems have largely been limited to 1-D scalar problems (*e.g.* heat flow) and 1-D beam problems [12]. Bhaskaran and Berkooz [10] present an FEM-based continuous sensitivity solution for a 2-D structural elasticity problem that is also considered in [13], but there remains a dearth of structural elasticity applications that employ continuous sensitivity methods. Pelletier *et al.* have employed continuous sensitivity methods for a range of fluid-structure interaction problems [14-16] with prominent success, however much of their work focuses on flow variable sensitivities. To the authors' knowledge, this is the first example in the literature that employs least-squares formulations to solve the CSE system for a coupled fluid-structure system as well as the first nonlinear, transient gust sensitivity solution. Additionally, very few applications of CSE methods to transient problems exist in the literature.

Continuous sensitivity systems are typically posed in terms of local derivatives (an Eulerian reference frame), though it is possible to derive the CSE system in total derivative form (Lagrangian reference frame [17]). For shape optimization of fluid applications, an Eulerian description of the flow sensitivity is usually adequate. Thus, much of the literature does not emphasize the distinction between the local and total derivative. For structural optimization problems, however, the design sensitivity at a material point is usually required, which necessitates a means to convert the local sensitivities from the CSE solution to total sensitivities at a given material point. We describe this conversion and present a simple example that illustrates the distinction between the local and total derivatives.

Currently, the most common and widely applied approaches for solving fluid-structure interaction (FSI) problems use different theoretical formulations and numerical methods to solve the fluid and structure problems separately, a method that can be fraught with convergence issues and inaccurate solutions when the method does converge [18, 19]. A more significant drawback is that when applied to (numerical approximate) sensitivity applications, the iterative nature of the segregated strategy may require multiple computationally expensive cycles for every variation of an individual design variable. If scaled to hundreds or thousands of design variables, the segregated method is computationally intractable for numerical approximate methods. Alternative FSI solution strategies casts the coupled fluid, structure, and mesh deformation systems as a single monolithic or fully-coupled fluid-structure-mesh formulation [20-22]. This approach generally gives faster convergence [23], though the memory requirements are substantially greater since the fluid, structure, and mesh degrees of freedom must be treated and solved simultaneously. As overall computer performance improves and the expense of large memory approaches decreases, the trend in aeroelastic computational methods is towards full coupling of the fluid-structure-mesh systems [24, 25], though there are still several open research questions regarding the proper weighting between the different physics and interface between the separate fluid and structure domains.

A least-squares finite element method (LSFEM) formulation for the FSI problem is promising in that it provides a consistent approach with the same numerical framework for the simultaneous solution of the fully-coupled fluid, structure , and accompanying mesh deformation problems [26, 27]. The LSFEM method is in the class of weighted residual variational solutions to partial differential equations and has seen a renaissance of interest in the last several years: [27-35] are representative of the range of applications to both fluid and structural problems. A LSFEM approach seeks to minimize the L^2 norm of the residual error of the governing differential equations. Least-squares methods for time-dependent and nonlinear problems are well-established in the literature [29], and appear applicable to analysis of transient, nonlinear gust response. Gust response loads are of particular interest as they have been identified as the critical load condition for several proposed aerospace applications, including a next-generation, long-endurance vehicle designed for persistent intelligence, surveillance, and reconnaissance missions [36, 37].

This paper begins with a derivation of the continuous sensitivity system and its associated boundary conditions. The next section describes a fluid-structure problem that is fairly simple to describe and solve yet complex enough to capture all the salient aspects of a continuous sensitivity calculation for a coupled domain, nonlinear, transient system. This is followed by a brief description of the LSFEM computational approach used to solve both the transient, nonlinear fluid-structure system and the CSE system. The form of the linear CSE system is described and contrasted with the form of the nonlinear fluid-structure system. The sensitivity conversion between the local and total derivatives is demonstrated and shape parameter gradients are used to extrapolate the transient response to a design variation of the problem. The results are compared with both finite difference calculations and numerical solutions of the perturbed system.

II. Continuous Sensitivity Equations

Consider the following general boundary value system defined in a domain Ω with a boundary Γ for which we seek a solution $\mathbf{u}$ of the equations

$$\mathbf{Au} = \mathbf{f} \text{ in } \Omega \tag{1}$$

$$\mathbf{Bu} = \mathbf{g} \text{ on } \Gamma \tag{2}$$

where $\mathbf{A}$ is a first-order time-space differential operator given by

$$\mathbf{A} = \mathbf{A}_t \frac{\partial}{\partial t} + \sum_{i=1}^{\dim} \mathbf{A}_i \frac{\partial}{\partial x_i} + \mathbf{A}_0 \tag{3}$$

and, $\mathbf{B}$ is the boundary condition operator

$$\mathbf{B} = \mathbf{B}_t \frac{\partial}{\partial t} + \sum_{i=1}^{\dim-1} \mathbf{B}_i \frac{\partial}{\partial \xi_i} + \mathbf{B}_0 \tag{4}$$

Here ξ denote the coordinates that parameterize the boundary. The first forward difference for calculating the sensitivity of the solution with respect a design parameter, *b*, is

$$\Delta_b(\mathbf{u}) = \frac{\mathbf{u}(b+\delta b) - \mathbf{u}(b)}{\delta b} \tag{5}$$

Besides the computational expensive involved in solving the system twice, a challenge in finite difference methods is in determining the optimum step size, δb. Large steps are dominated by truncation error (which can be significant if the system is nonlinear) and small steps are dominated by numerical round-off error. The continuous sensitivity method avoids the numerical shortcomings of finite difference methods by differentiating the field equations (1-2) to yield a governing continuous system of equations for the desired sensitivity variables. For example, differentiating a transient, two-dimensional domain system with respect to a design parameter, *b*, yields

$$\frac{\partial}{\partial b}\left[\mathbf{A}_0(\mathbf{u};b)\mathbf{u} + \mathbf{A}_1(\mathbf{u};b)\mathbf{u}_{,x} + \mathbf{A}_2(\mathbf{u};b)\mathbf{u}_{,y} + \mathbf{A}_t(\mathbf{u};b)\mathbf{u}_{,t}\right] = \frac{\partial}{\partial b}\left[\mathbf{f}(\mathbf{x};b)\right] \tag{6}$$

where the subscripted comma notation denotes partial differentiation. Equation (6) can be expanded as

$$\mathbf{A}_{0,b}\mathbf{u}_{,b}\mathbf{u} + \mathbf{A}_0\mathbf{u}_{,b} + \mathbf{A}_{1,b}\mathbf{u}_{,b}\mathbf{u}_{,x} + \mathbf{A}_1\mathbf{u}_{,xb} + \mathbf{A}_{2,b}\mathbf{u}_{,b}\mathbf{u}_{,y} + \mathbf{A}_2\mathbf{u}_{,yb} + \mathbf{A}_{t,b}\mathbf{u}_{,b}\mathbf{u}_{,t} + \mathbf{A}_t\mathbf{u}_{,tb} = \mathbf{f}_{,b}(\mathbf{x};b) \tag{7}$$

Since the spatial-temporal derivatives are independent operations from the sensitivity derivative, the order of differentiation may be reversed. Note that this commutation of differentiation is not possible if the sensitivity derivative in (6) is not a local derivative [6]. Collecting sensitivity terms yields the continuous sensitivity system

$$\left[\mathbf{A}_0 + \mathbf{A}_{0,b}\mathbf{u} + \mathbf{A}_{1,b}\mathbf{u}_{,x} + \mathbf{A}_{2,b}\mathbf{u}_{,y} + \mathbf{A}_{t,b}\mathbf{u}_{,t}\right]\mathbf{u}_{,b} + \mathbf{A}_1(\mathbf{u}_{,b})_{,x} + \mathbf{A}_2(\mathbf{u}_{,b})_{,y} + \mathbf{A}_t(\mathbf{u}_{,b})_{,t} = \mathbf{f}_{,b}(\mathbf{x};b) \tag{8}$$

Notice that (8) is in the same form as (1) with (3) operating on the sensitivity variable $\mathbf{u}_{,b}$ instead of the original field variable $\mathbf{u}$, provided that the first bracketed matrix term in (8) is identified as the ${}^b\mathbf{A}_0$ sensitivity matrix. The gradient operators, $\mathbf{A}_1$, $\mathbf{A}_2$, and $\mathbf{A}_t$, are unchanged for the CSE system. For linear systems with *b* representing a boundary shape parameter, the $\mathbf{A}_{i,b}$ terms in (8) vanish and the component CSE operators are identical to the original system operators. Also note that the continuous sensitivity system is always linear in the sensitivity variable, $\mathbf{u}_{,b}$, even when the original system is nonlinear.

The boundary conditions of the sensitivity equation specify how the sensitivity variables behave on the boundary of the domain. Thus, analogous to the approach used above, the sensitivity of boundary operator system may be written as a CSE system

$$\left[\mathbf{B}_0 + \mathbf{B}_{0,b}\mathbf{u} + \mathbf{B}_{\xi,b}\mathbf{u}_{,\xi}\right]\mathbf{u}_{,b} + \mathbf{B}_{\xi}(\mathbf{u}_{,b})_{,\xi} = \mathbf{g}_{,b}(\mathbf{x};b) \quad \text{on } \Gamma(b) \tag{9}$$

We introduce a superscript prefix notation, ${}^b\mathbf{u}$, to denote the sensitivity variable that is determined by solving the CSEs. This is distinct from an analytic sensitivity, denoted by $\mathbf{u}_{,b}$, which is used to represent the sensitivity determined by taking the derivative of an analytic solution $\mathbf{u}$ to equations (1-2). We also introduce notation for the finite difference operator, $\Delta_b(\mathbf{u})$, given by (5), and the material derivative operator, $D_b(\mathbf{u})$, defined below.

Thus, the continuous sensitivity system is simply another system of differential equations, which, given with the appropriate boundary data, represents a well-posed boundary value problem that may be solved by a wide variety of numerical approaches. It is convenient in many cases to use the same numerical method and framework to solve the sensitivity system as was used to solve the original system.

For shape variation problems, the boundary Γ is a function of the design parameter b and the evaluation of (9) must account for the total variation of a material point on the boundary. The Eulerian and material points are related through the total (material) derivative

$$D_b(u) \equiv \left.\frac{Du}{Db}\right|_{\mathbf{X}} = \left.\frac{\partial u}{\partial b}\right|_{\mathbf{x}} + \nabla u \cdot \left.\frac{\partial \mathbf{X}_\Omega}{\partial b}\right|_{\mathbf{X}} \tag{10}$$

where $D_b(\cdot)$ is the material derivative operator with respect to the parameter b, $\mathbf{X}$ denotes a material coordinate and $\mathbf{x}$ denotes a spatial coordinate (Eulerian description). Thus the total derivative of u with respect to b at a material point $\mathbf{X}$ consists of the local derivative of u with respect to parameter b and the convective transport term which accounts for how the material point $\mathbf{X}$ moves as the design parameter b varies. If u is a vector quantity, then the gradient operation and dot product in the transport term are carried out component-wise. Solving (10) for the local derivative gives the desired sensitivity variable boundary condition for the CSE system in terms of the local derivatives ${}^b\mathbf{u}$

$${}^b\mathbf{u}\big|_\Gamma \equiv \left.\frac{\partial \mathbf{u}}{\partial b}\right|_{\mathbf{X}=\Gamma} = \left.\frac{D\mathbf{u}}{Db}\right|_\Gamma - \nabla \mathbf{u} \cdot \frac{\partial \mathbf{X}_{\Gamma(b)}}{\partial b} \tag{11}$$

where in 2-D

$$\mathbf{X}_{\Gamma(b)} = \left\{(x, y) \in \Gamma(b)\right\} \tag{12}$$

are coordinates (ordered pairs in $\mathbf{R}^2$) that define the boundary as a function of b. The first term on the right side of (11) accounts for how the boundary conditions for the problem change with respect to the design parameter. In most cases, this term is zero. That is, the boundary condition does not often change as the shape changes. The convection term is the dot product of the derivative of the set of spatial coordinates that define the boundary with the gradient of the solution to (1), where for vectors, the gradient operation is carried out row-wise.

To summarize, the continuous sensitivity system is a linear boundary value problem derived by taking the derivatives of the original field equations, (1-2). The set of sensitivity boundary condition data are of the same form as for the original problem; however, the boundary shape variation for shape sensitivity problems must be accounted for through (11). The continuous sensitivity equations may be derived in either total or local derivative form. When expressed in local form, only the boundary parameterization need be described. In total derivative form, the parameterization or transformation function for the entire domain is necessary which is equivalent to having to solve the mesh Jacobian. The domain Jacobian must also be solved and inverted for continuous sensitivity domain parameterization (total derivative) methods [6]. Posing the CSE in local derivative form and parameterizing the boundary as described above avoids the numerical complexity and expense of the mesh and domain Jacobian. Next we illustrate how to relate the local and total derivative sensitivity forms for a particular example.

III. Sting Mounted Typical Section Gust Model

Consider a NACA 0012 airfoil shape mounted on a flexible sting (Figure 2). The sting is modeled as a nonlinear Euler-Bernoulli beam capable of large deflections. At a positive angle of attack, the airfoil generates lift, deflecting the beam in the fluid resulting in an increased angle of attack. Equilibrium deflection of the sting occurs when the force and moments generated by the lifting airfoil balance the internal sting force and moments resisting the bending. The transient response to a discrete gust front flowing past the airfoil is modeled and evaluated. Fluid forces and moments on the airfoil are calculated using quasi-steady flow aerodynamics for a thin airfoil. Although, physically realistic fluid forces depend on the unsteady aerodynamics of the moving airfoil, we accept the physical limitations of not including unsteady effects, since we are primarily interested in demonstrating continuous sensitivity analysis of a transient, coupled problem. The physical simplicity of quasi-steady aerodynamics is attractive and sufficient for this objective.

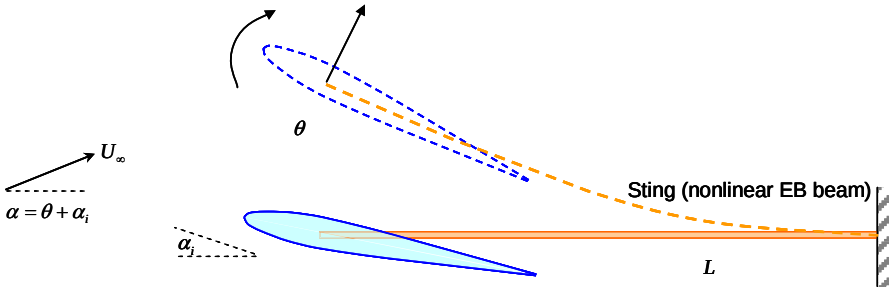

Figure 2: Flexible sting mounted airfoil

Taking the length of the sting as a shape parameter, we calculate the sensitivity of the coupled fluid-structure variables to sting length. The left and right boundaries of the sting, the *tip* and *root*, are naturally parameterized with respect to beam length as

$$\mathbf{X}_{tip} = \{0\} \quad , \quad \mathbf{X}_{root} = \{L\} \tag{13}$$

To convert the local sensitivities into a total derivative, we must define a domain transformation function that is compatible with the FSI boundary data. An obvious choice, represented in Figure 3, defines the material points of the domain by

$$\mathbf{X}_\Omega(x) = \{\xi L \,|\, \xi = x/L;\ \xi \in [0,1]\} \tag{14}$$

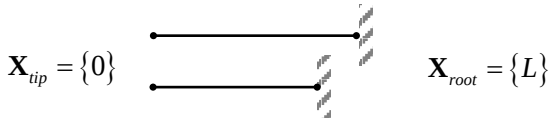

Figure 3: Sting length boundary parameterization

A. Typical Section Fluid Model

The force due to lift produced by the airfoil is modeled using thin-airfoil theory is

$$F_f = q_\infty C_{L_\alpha} \alpha_e \tag{15}$$

where q_∞ is the freestream dynamic pressure, C_{L_α} is the airfoil lift curve slope, and α_e is the effective angle of attack. For the sting-mounted airfoil problem in Figure 2 the effective angle of attack is a function of the angle of incidence, α_i, the rotation of the beam tip, θ_{tip}, the relative change in angle of attack due to airfoil dynamic motion, and the component change due to gust direction. The complete typical section fluid force model is

$$F_f = q_\infty C_{L_\alpha} \left(\alpha_i + \theta_{tip} - \eta \frac{\dot{v}_{tip}}{U_\infty} + \frac{V_g}{U_\infty} \right) \tag{16}$$

where η is an efficiency parameter for the plunge rate damping term, $\dot{v}_{tip}/U_\infty$, $\dot{v}_{tip}$ is the velocity of the tip of the beam, U_∞ is the freestream velocity, and V_g is the time-dependent gust velocity. The vertical gust is modeled using the usual discrete gust idealization of a *one-minus-cosine* pulse [38], so that

$$V_g(t) = \begin{cases} \frac{1}{2} V_{g,\max} \left(1 - \cos \dfrac{2\pi(t - \tau_0)}{T_g} \right) & \tau_0 \le t \le T_g \\ 0 & o.w. \end{cases} \tag{17}$$

where $V_{g,\max}$ is the maximum amplitude of the gust, τ_0 is the start of the gust, and T_g is the duration of the gust. Since the NACA 0012 is symmetric and the tip of the sting is mounted at the aerodynamic center of the airfoil, the fluid moments are zero.

$$M_f = 0 \tag{18}$$

This model ignores unsteady aerodynamic effects and the time it takes for the gust to transit the chord of the airfoil, but it is sufficient for the purpose of demonstrating the pertinent steps in a least-squares continuous sensitivity analysis.

The gust is not a function of beam length, so that

$$\frac{\partial}{\partial L} V_g(t) = 0 \tag{19}$$

Likewise, the angle of incidence is not a function of beam length. Differentiating the governing fluid equation, (16), with respect to beam length yields the sensitivity equation for the typical section fluid force and moment sensitivity

$${}^{L}F_f = q_\infty C_{L_\alpha} \left({}^{L}\theta_{tip} - \eta \frac{{}^{L}\dot{v}_{tip}}{U_\infty} \right) \tag{20}$$

$${}^{L}M_f = 0 \tag{21}$$

B. Euler-Bernoulli Beam

The sting is modeled as a nonlinear Euler-Bernoulli beam where the nonlinear von Karman strain relations account for possible large deflections of the beam. The Euler-Bernoulli assumptions that plane sections remain plane after deformation are equivalent to neglecting the Poisson effect and transverse strains and is adequate for the long slender sting in this problem. Further, only transverse loading conditions will be considered. The force and free-body diagram of the beam is given in Figure 4.

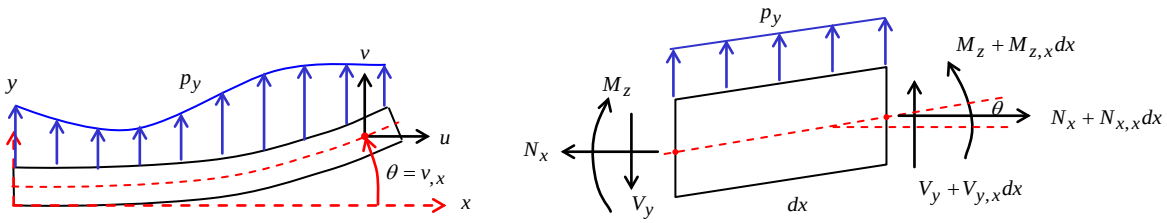

Figure 4: Beam free-body diagram

With the Euler-Bernoulli assumption, the angle of rotation and the internal bending moment are given by

$$\theta = v_{,x} \tag{22}$$

$$M_z = EI\theta_{,x} \tag{23}$$

where v is the vertical displacement, and the product of Young's modulus, E, and the moment of inertia, I, is the effective bending stiffness of the beam. The axial force, N_x, at any cross section of the beam is given by

$$N_x = \int_A \sigma_{xx} dA \tag{24}$$

where σ_{xx} is the normal stress and A is the cross sectional area of the beam. Summing the moments about the z-axis yields and neglecting rotary inertia

$$M_{z,x} + V_y - N_x\theta = 0 \tag{25}$$

The nonlinear von Karman strain-displacement relation [39]in the axial direction is

$$\varepsilon_{xx} = u_{,x} + \tfrac{1}{2}\theta^2 \tag{26}$$

which in the absence of axial loads (so that $u_{,x} = 0$) and together with the constitutive equation

$$\sigma_{xx} = E\varepsilon_{xx} \tag{27}$$

yields the nonlinear relationship between shear, bending moment, and rotation

$$M_{z,x} + V_y - \frac{EA}{2}\theta^3 = 0 \tag{28}$$

Note that V_y is the shear force perpendicular to the x-axis, not the shear force, Q, perpendicular to the neutral axis of the deformed beam which is given by

$$Q = -V_y + \frac{EA}{2}\theta^3 \tag{29}$$

Finally, summing the forces in the y-direction yields the final equation governing the beam dynamics

$$\rho_y \frac{\partial^2 v}{\partial t^2} - V_{y,x} = p_y \tag{30}$$

where ρ_y is the mass per unit length of the sting and p_y is the transverse load per unit length. A lumped mass is also included at the tip of the airfoil to represent the mass of the airfoil. Substituting (28) and (23) into (30) yields the nonlinear governing equation large deflections, v, of the sting subject to a transverse load

$$\rho_y \frac{\partial^2 v}{\partial t^2} + \frac{\partial^2}{\partial x^2}\left(EI\frac{\partial^2 v}{\partial x^2}\right) - \frac{\partial}{\partial x}\left[\frac{EA}{2}\left(\frac{\partial v}{\partial x}\right)^3\right] = p_y \tag{31}$$

For ease in formulating (31) in a least-squares finite element model, we express the nonlinear beam system in first-order matrix operator form

$$A_t \mathbf{u}_{,t} + A_0 \mathbf{u} + A_1 \mathbf{u}_{,x} = \mathbf{f} \tag{32}$$

where $\mathbf{u} = \begin{bmatrix} v & \theta & M_z & V_y & \dot{v} \end{bmatrix}^T$ and the matrix operators are

$$A_t = \begin{bmatrix} 0 & 0 & 0 & 0 & 0 \\ 0 & 0 & 0 & 0 & 0 \\ 0 & 0 & 0 & 0 & 0 \\ 0 & 0 & 0 & 0 & \rho_y \\ 1 & 0 & 0 & 0 & 0 \end{bmatrix} \quad A_0 = \begin{bmatrix} 0 & 1 & 0 & 0 & 0 \\ 0 & 0 & 1/EI & 0 & 0 \\ 0 & \frac{1}{2}EA\theta^2 & 0 & -1 & 0 \\ 0 & 0 & 0 & 0 & 0 \\ 0 & 0 & 0 & 0 & -1 \end{bmatrix} \quad A_1 = \begin{bmatrix} -1 & 0 & 0 & 0 & 0 \\ 0 & -1 & 0 & 0 & 0 \\ 0 & 0 & -1 & 0 & 0 \\ 0 & 0 & 0 & 1 & 0 \\ 0 & 0 & 0 & 0 & 0 \end{bmatrix} \quad \mathbf{f} = \begin{bmatrix} 0 \\ 0 \\ 0 \\ p_y \\ 0 \end{bmatrix} \tag{33}$$

The system of continuous sensitivity equations is formed by differentiating (22), (23), (28), and (30). Thus the CSEs in first order form for the nonlinear beam are

$${}^L\theta = {}^L v_{,x} \tag{34}$$

$${}^L M_z = EI\,{}^L\theta_{,x} \tag{35}$$

$${}^L M_{z,x} + {}^L V_y - \tfrac{3}{2}EA\theta^2\left({}^L\theta\right) = 0 \tag{36}$$

$$\rho_y \left({}^L\dot{v} \right) - {}^L V_{y,x} = {}^L p_y \tag{37}$$

$${}^L\dot{v} = {}^L v_{,t} \tag{38}$$

As noted above, the sensitivity system is linear, even though the original elasticity equations were nonlinear. In first-order, matrix operator form, (34)-(38) are

$$A_t = \begin{bmatrix} 0 & 0 & 0 & 0 & 0 \\ 0 & 0 & 0 & 0 & 0 \\ 0 & 0 & 0 & 0 & 0 \\ 0 & 0 & 0 & 0 & \rho_y \\ 1 & 0 & 0 & 0 & 0 \end{bmatrix} \quad A_0 = \begin{bmatrix} 0 & 1 & 0 & 0 & 0 \\ 0 & 0 & 1/EI & 0 & 0 \\ 0 & \frac{3}{2}EA\theta^2 & 0 & -1 & 0 \\ 0 & 0 & 0 & 0 & 0 \\ 0 & 0 & 0 & 0 & -1 \end{bmatrix} \quad A_1 = \begin{bmatrix} -1 & 0 & 0 & 0 & 0 \\ 0 & -1 & 0 & 0 & 0 \\ 0 & 0 & -1 & 0 & 0 \\ 0 & 0 & 0 & 1 & 0 \\ 0 & 0 & 0 & 0 & 0 \end{bmatrix} \quad \mathbf{f} = \begin{bmatrix} 0 \\ 0 \\ 0 \\ p_y \\ 0 \end{bmatrix} \tag{39}$$

Note that, as explained above, the A_t and A_1 CSE matrix operators are the same as the original, nonlinear elasticity system, but that the A_0 matrix for the CSE system is different.

C. Coupled fluid-structure solution

The typical section fluid model and beam sting model are coupled through the dependance of the airfoil angle of attack on the sting tip rotation and the beam tip force and moment on the aerodynamic forces. The fluid-structure interface condition for the FSI problem is given by the balance of forces at the tip of the beam

$$F_f = -V_y\big|_{tip} \tag{40}$$

$$M_f = M_z\big|_{tip} \tag{41}$$

The derivatives of the fluid-structure interface conditions yield the fluid-structure sensitivity equation interface relations

$${}^L F_f = -{}^L V_y\big|_{tip} \tag{42}$$

$${}^L M_f = {}^L M_z\big|_{tip} \tag{43}$$

The complete coupled fluid-structure model problem boundary and initial conditions for the FSI problem are given in Table 1 and the corresponding boundary and initial conditions for the CSE problem are given in

Table 1 Sting-mounted airfoil FSI problem boundary conditions

Boundary	Constrained dofs	
fluid IC	$\theta = 10^\circ \quad \dot{v} = 0$	steady equilibrium
beam IC	$\dot{v} = 0$	steady equilibrium
beam root BC	$v = 0 \quad \theta = 0 \quad \dot{v} = 0$	clamped
beam tip interface	$V_y(t) = F_f\left(\theta, \dot{v}, V_g(t)\right) \quad M_z = 0$	fluid-structure interface (force equilibrium)

Table 2 Sting-mounted airfoil CSE problem boundary conditions

Boundary	Constrained dofs	
beam IC	${}^{L}\dot{v} = 0$	steady equilibrium
beam root BC	${}^{L}v = -v_{,x} \quad {}^{L}\theta = -\theta_{,x} \quad {}^{L}\dot{v} = -\dot{v}_{,x}$	clamped
beam tip interface	${}^{L}V_y(t) = -{}^{L}F_f \quad {}^{L}M_z = 0$	fluid-structure interface (force equilibrium)

IV. Least-Squares Finite Element Method

The LSFEM model is based on the idea of minimization of the norm of the residual (or error) in the governing differential equations due to the approximation of the variables in the equations. The weighted sum of the squares of the system residuals defines the least-squares functional

$$J(\mathbf{u};\mathbf{f},\mathbf{g}) = \left\|\mathbf{Au} - \mathbf{f}\right\|_{\Omega}^{2} + \alpha_{\Gamma}\left\|\mathbf{Bu} - \mathbf{g}\right\|_{\Gamma}^{2} \tag{44}$$

where α_{Γ} is a relative weighting parameter for the residual of error in the boundary condition and the residual of the governing differential equation (both expressed in terms of the L^2 norm). Equation (44) represents a weak enforcement (i.e., integral sense) of the boundary conditions. The boundary conditions could alternatively be imposed directly on the boundary degrees of freedom (strong enforcement of the boundary conditions). A necessary condition for **u** to minimize (44) is that the first variation of (44) vanishes at **u** [40]. This yields an equivalent bilinear-linear inner product form [41] for the boundary value system (1)-(2)

$$B(\mathbf{u},\mathbf{v}) = l(\mathbf{f},\mathbf{v}) \qquad \forall \mathbf{v} \in \mathbf{V} \tag{45}$$

where the bilinear-linear inner product form for the domain is

$$\begin{aligned} B_{\Omega}(\mathbf{u},\mathbf{v}) &\equiv (\mathbf{Au},\mathbf{Av}) \\ l_{\Omega}(\mathbf{f},\mathbf{v}) &\equiv (\mathbf{f},\mathbf{Av}) \end{aligned} \tag{46}$$

and the bilinear-linear inner product form for the boundary is

$$\begin{aligned} B_{\Gamma}(\mathbf{u},\mathbf{v}) &\equiv (\mathbf{Bu},\mathbf{Bv}) \\ l_{\Gamma}(\mathbf{g},\mathbf{v}) &\equiv (\mathbf{g},\mathbf{Bv}) \end{aligned} \tag{47}$$

For nonlinear operators, the bilinear-linear form is based on iterated succesive approximations to the solution **u**. The The domain will be partitioned into finite elements and in each element, we approximate the solution **u** by

$$\mathbf{u} \approx \mathbf{u}_h^e = \sum_{j=1}^{n_{dof}^e} \psi_j \left[u_1 \ldots u_{n_{nodes}} \quad a_1 \ldots a_{n_a} \quad b_1 \ldots b_{n_a} \right]^T \tag{48}$$

where ψ_j are higher-order hierarchal shape functions [42]. For the *p*-element solutions presented below, we employ Szabo's quadrilateral shape function expansion basis [43], a serendipity expansion built of kernel functions constructed from Legendre polynomials. The element degrees of freedom, $n_{dof}^e = n_{nodes} + n_a + n_b$, consist of the element nodal values, $u_1 \ldots u_{n_{nodes}}$, the edge coefficients, $a_1 \ldots a_{n_a}$, and the interior (bubble) mode coefficients, $b_1 \ldots b_{n_a}$.

Substituting (48) into (46) and (47) yields n_{dof}^{e} algebraic equations

$$\left[\mathbf{K}^{e}+\alpha_{\Gamma}\mathbf{K}_{\Gamma}^{e}\right]\mathbf{u}=\mathbf{F}^{e}+\alpha_{\Gamma}\mathbf{G}^{e} \tag{49}$$

The element stiffness matrices and equivalent force vectors are defined by

$$\mathbf{K}^{e}=\int_{\Omega^{e}}\left(\mathbf{A}\psi_{1},...,\mathbf{A}\psi_{n_{dof}^{e}}\right)^{T}\left(\mathbf{A}\psi_{1},...,\mathbf{A}\psi_{n_{dof}^{e}}\right)d\Omega \tag{50}$$

$$\mathbf{F}^{e}=\int_{\Omega^{e}}\left(\mathbf{A}\psi_{1},...,\mathbf{A}\psi_{n_{dof}^{e}}\right)^{T}\mathbf{f}\;d\Omega \tag{51}$$

$$\mathbf{K}_{\Gamma}^{e}=\int_{\Gamma^{e}}\left(\mathbf{B}\psi_{1},...,\mathbf{B}\psi_{n_{dof}^{e}}\right)^{T}\left(\mathbf{B}\psi_{1},...,\mathbf{B}\psi_{n_{dof}^{e}}\right)d\Gamma \tag{52}$$

$$\mathbf{G}^{e}=\int_{\Gamma^{e}}\left(\mathbf{B}\psi_{1},...,\mathbf{B}\psi_{n_{dof}^{e}}\right)^{T}\mathbf{g}\;d\Gamma \tag{53}$$

The element stiffness and load vectors are assembled into a global system of equations, which has the form

$$\left[\mathbf{K}+\alpha_{\Gamma}\mathbf{K}_{\Gamma}\right]\mathbf{u}=\mathbf{F}+\alpha_{\Gamma}\mathbf{G} \tag{54}$$

The LSFEM approach is attractive for fluid-structure interaction problems since it permits a single numerical approach to solving the governing domain and interaction equations without special treatment of the disparate physics of the fluid and structure domains. The LSFEM also permits stable mixed elements for structural elasticity that are not restricted by the LBB condition. Mixed formulations for the elasticity system are preferred to strict displacement formulation elements, since they allow direct access to the stress variables for application of fluid pressure interaction conditions and the calculation of stress sensitivities at the fluid-structure interface.

V. Transient Gust Response and Sensitivity Solution

The nonlinear, transient gust response of the sting-mounted NACA 0012 airfoil is solved using a successive substitution nonlinear convergence outer loop around a time-space, least-squares finite element model of the transient system. The typical section fluid model is a single degree of freedom model and the nonlinear Euler-Bernoulli beam is a five degree of freedom model with only one spatial dimension. This readily permits time as the second dimension in an endemic LSFEM research code. The nonlinear convergence for the beam tip deflection, velocity, and rotation to a 1 sec *one-minus-cosine* gust is plotted in Figure 5. Taking beam length as a shape design parameter, we solve the continuous sensitivity system for the fluid and structure state variable sensitivities to beam length. The boundary conditions for the continuous sensitivity system are determined using (11) from the least-squares solution to the fluid-structure system as well as the boundary parameterization given by (13). The continuous sensitivity system is solved using the same LSFEM code and computational mesh used for the FSI system. The LS-CSE solution for the tip of the beam as a function of time is plotted in Figure 6. Recall, that the CSE system is always a linear boundary value problem, even when the underlying problem is nonlinear. Figure 6 plots the sensitivity solution based on both a linear solution to the underlying FSI problem and the nonlinear solution to the FSI problem. As evident in Figure 5, the nonlinear effects of the system are only significant at large beam deflections and rotations. Because the geometric nonlinearities result in a stiffening of the beam, the sensitivities at times associated with large response are reduced for the LS-CSE solution based on the nonlinear FSI solution.

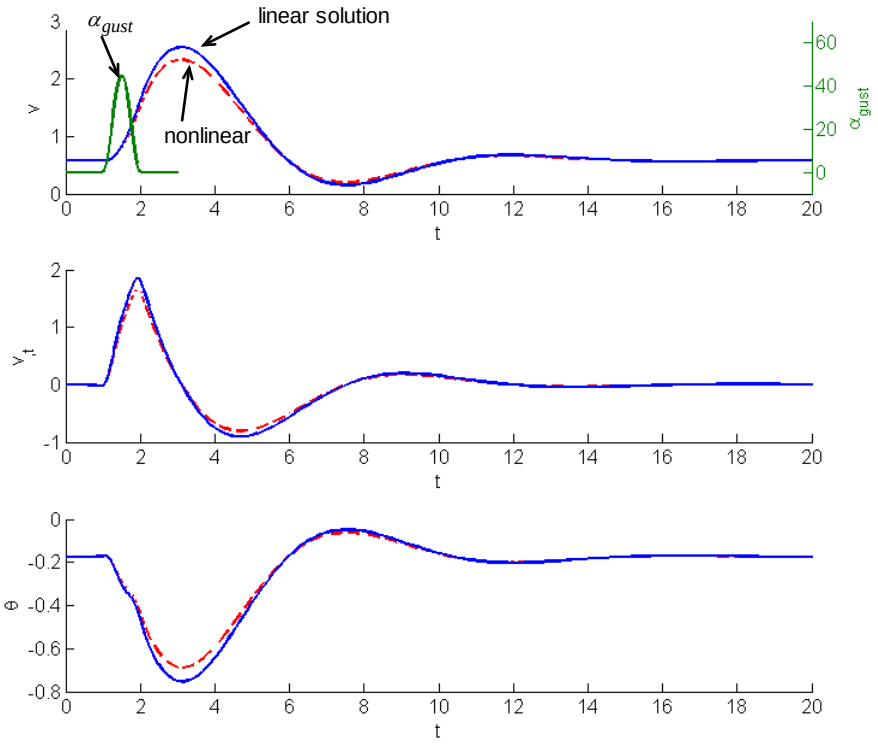

Figure 5: Beam tip deflection, velocity, and rotation nonlinear transient response to a 1 sec *one-minus-cosine* gust

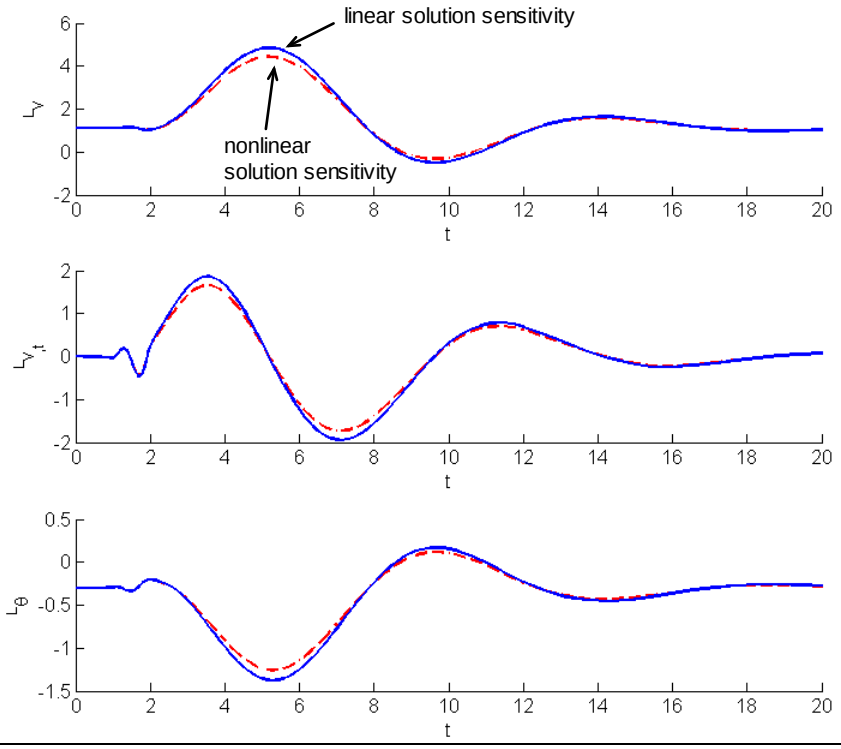

Figure 6: Transient gust sensitivity to beam length for beam tip deflection, velocity, and rotation

The total material derivative sensitivity is calculated by adding the convection term from the original solution to the LS-CSE results, (10). Structural optimization methods are usually based on gradients determined from total derivatives at given material points, thus the total derivative form of the CSE solution is generally desired. Note that finite difference results are by nature approximations to total derivatives. A comparison of the total derivative LS-CSE solution and the finite difference sensitivity for the nonlinear, transient gust response is plotted in Figure 7.

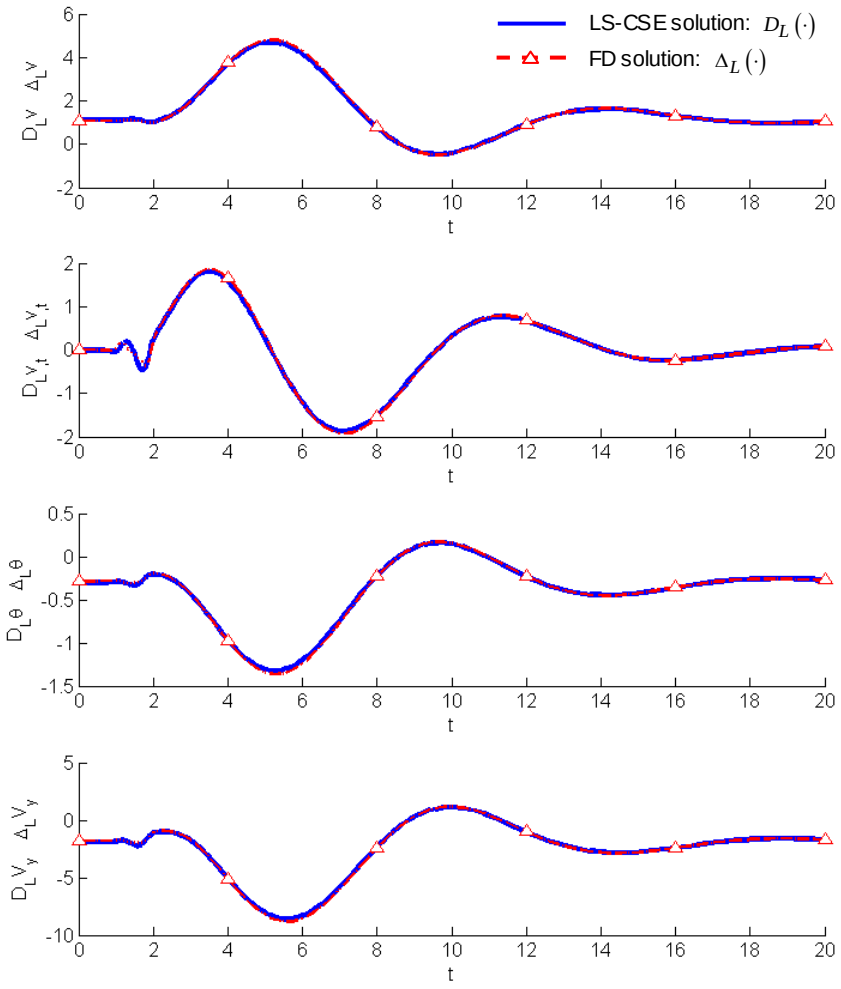

Figure 7: Comparison of finite difference and LS-CSE solution for beam deflection, velocity, rotation, and internal shear sensitivity to the beam length for a 1 sec *one-minus-cosine* gust

Since the LS-CSE solution yields the design parameter sensitivity of all the state variables, single or multi-variable optimization methods requiring gradient information can be accomplished with respect to any of the state variables. For example, a multi-objective optimization could be done to minimize the beam root bending moment while maintaining limits on maximum deflection and rotation of the sting. As another example of a possible use of the sensitivity solution, consider the extrapolation of the nonlinear beam deflection for the transient gust problem at a particular point in time. For example, at $t = 3$, the beam tip deflection and rotation of the FSI solution in Figure 5 is close to a maximum. The LS-CSE solution of the entire beam at $t = 3$ is given in Figure 8. Note that the entire transient CSE problem does not have to be solved if only the sensitivity at a point in time is desired. The CSE boundary conditions for the sensitivity at $t = 3$ only depend on the nonlinear FSI solution at $t = 3$ and not on any of

the prior history of the transient CSE system. From a first-order Taylor series approximation, the extrapolated beam deflection and rotation at any point in time is

$$v\left(x;L_0+\delta L\right)\approx v\left(x;L_0\right)+D_L v\left(x;L_0\right)\delta L \tag{55}$$

and

$$\theta\left(x;L_0+\delta L\right)\approx \theta\left(x;L_0\right)+D_L \theta\left(x;L_0\right)\delta L \tag{56}$$

where L_0 is the nominal beam length and the total material sensitivity is given by (10). Explicitly, the total sensitivity for deflection is

$$D_L v\left(x;L_0\right)={}^{L}v\left(x;L_0\right)+v_{,x}\left(x;L_0\right)\frac{x}{L_0} \tag{57}$$

where ${}^{L}v$ is the LS-CSE solution sensitivity variable, and the spatial gradient of deflection in the convection term comes from the nonlinear FSI solution. The extrapolated deflections and rotations at t = 3 sec for a 3% and 6% longer beam are calculated and compared with the actual beam deflections and rotations in Figure 9. The agreement for a 3% longer beam is fairly close and the extrapolation for a 6% longer beam is noticeably more inaccurate. This is due to the limited accuracy of the first-order Taylor series to a system that is not first-order. For the parameters modeled in this FSI system, the static margin for divergence is less than 10% for a 6% longer beam compared to 30% for the original beam. This results in increasingly large deflections for relatively small perturbations in beam length.

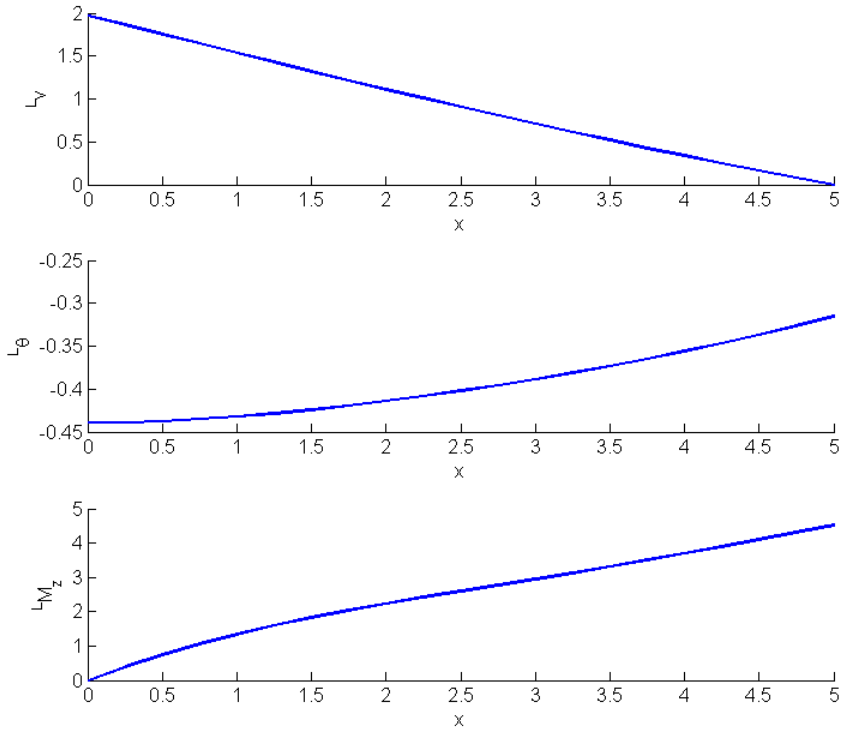

Figure 8: Beam deflection, rotation, and internal moment sensitivity to the nonlinear gust response at t = 3

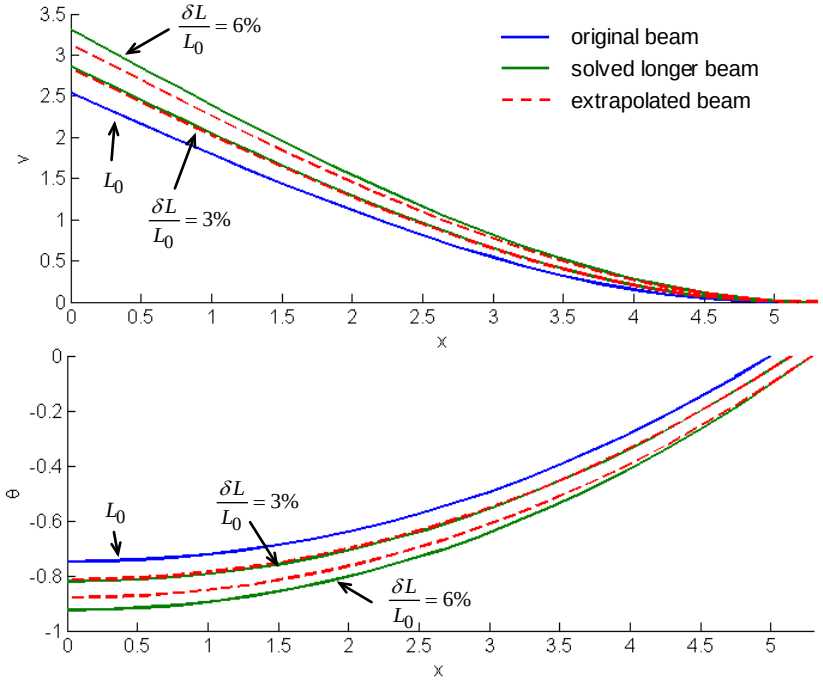

Figure 9: Extrapolated and actual beam deflection and rotation to *one-minus-cosine gust* (t = 3 sec) for a 3% and 6% longer sting

VI. Conclusions

A least-squares formulation for solving the continuous sensitivity equations for shape sensitivity of transient, nonlinear fluid-structure problems was developed. For shape variation problems, a distinction should be made between the total material and local derivatives, particularly when the optimization is being carried with respect to material coordinates, as is usually the case for the design of structures subject to loads from immersed fluids. The local and total derivatives do not yield the same result, but it is possible to transform one into the other. Local sensitivities for shape variation problems are functions of the choice of transformation field or boundary parameterization, which are not unique. However, total derivatives, which are given at material coordinates, are unique. Thus, structural optimization methods should usually be based on gradients determined from total derivatives. The advantage of writing the CSE system in local derivative form is that only the boundary parameterization need be described, which avoids having to define a parameterization or transformation function for the entire domain. Thus, the CSE problem is generally simpler to pose and solve in term of local sensitivities and to then convert the result to total derivatives for optimization.

In the present work, the continuous sensitivity system was solved using the same high-order least-squares finite element method that was used to solve the underlying elasticity problem. The LSFEM approach is attractive in that it allows a stable mixed element, a better approximation of dual or secondary variable gradients compared to the weak form Galerkin formulations, an inherent error estimate, and flexibility in norm choice. The improved accuracy of the dual variable gradients inherent in the first-order mixed formulation is particularly important, since the gradients of the underlying solution are used to pose the boundary conditions for the sensitivity system. The higher-order p-element implementation also permitted a straightforward means to achieve a refined solution without needing a refined mesh. Thus, both the structural and sensitivity systems can be easily solved to any desired level of convergence using a single computational mesh per configuration. This is particularly important since, as observed in the literature, the CSE solution often requires different resolution than the original system.

The fluid model used in the current work was a relatively simple, single degree of freedom typical section model. Despite the simplicity of the model, the coupled fluid-structure system with structural system incorporating geometric nonlinearity exhibits rather complex transient response. The significance of the current work is in the definition of the coupled sensitivity system and the determination of the CSE boundary conditions. The nonlinear effect of the dynamic response for the underlying fluid-structure system was also demonstrated in the solution to the linear sensitivity system. Planned future work will incorporate more complicated fluid models. Overall, the least-squares continuous sensitivity method appears to be a promising option for the optimization of transient, nonlinear, fluid-structure optimization problems.

VII. Acknowledgements

The Air Force Office of Scientific Research (AFOSR) and the Air Force Research Laboratory (AFRL) Air Vehicles Directorate funded this research. The authors gratefully acknowledge the support of AFOSR program manager Dr. Fariba Fahroo and the AFRL Senior Aerospace Engineers Dr. Raymond Kolonay, Dr. Phillip Beran, and Dr. Maxwell Blair. The last author acknowledges support of the research by the Oscar S Wyatt Endowed Chair.

VIII. References

[1] Rasmussen, C., Canfield, R., and and Reddy, J.N., "Nonlinear Transient Gust Response Using a Fully- Coupled Least-Squares Finite Element Formulation," Vol. AIAA-2008-1821, 2008.

[2] Roberts, R.W., and Canfield, R.A., " Enriched Multipoint Cubic Approximations for Large-Scale Optimization," Vol. AIAA-2008-2146, 2008.

[3] Haug, E.J., Choi, K.K., and Komkov, V., "Design sensitivity analysis of structural systems," *Mathematics in science and engineering*, Vol. 177, Academic Press, Orlando, 1986.

[4] Choi, K.K., and Kim, N.H., "Structural sensitivity analysis and optimization," *Mechanical engineering series*, Springer Science+Business Media, New York, 2005.

[5] Dems, K., and Haftka, R.T., "Two Approaches to Sensitivity Analysis for Shape Variation of Structures," *Mech. Struct. & Mach.*, Vol. 16, No. 4, 1988-1989, pp. 501.

[6] Haftka, R.T., and Gürdal, Z., "Elements of structural optimization," *Solid mechanics and its applications*, Vol. 11, Kluwer Academic Publishers, Dordrecht ; Boston, 1992.

[7] Borggaard, J., and Burns, J., "A PDE Sensitivity Equation Method for Optimal Aerodynamic Design," *Journal of Computational Physics*, Vol. 136, 1997, pp. 366--384.

[8] Dems, K., and Mroz, Z., "Variational approach to first- and second-order sensitivity analysis of elastic structures," *International Journal for Numerical Methods in Engineering*, Vol. 21, 1985, pp. 637-661.

[9] Borggaard, J., and Burns, J., "A Sensitivity Equation Approach to Shape Optimization in FLuid Flows," Langley Research Center, NASA Contractor Report 191598 (ICASE Report No. 94-8), 1994.

[10] Bhaskaran, R., and Berkooz, G., "Optimization of Fluid-Structure Interaction using the Sensitivity Equation Approach," *Fluid-Structure Interaction, Aeroelasticity, Flow-Induced Vibrations and Noise*, Vol. 1, No. 53-1, 1997, pp. 49-56.

[11] Turgeon, E., Pelletier, D., and Borggaard, J., "A Continuous Sensitivity Equation Approach to Optimal Design in Mixed Convection," Vol. AIAA 99-3625, 1999.

[12] Stanley, L.G.D., and Stewart, D.L., "Design sensitivity analysis : computational issues of sensitivity equation methods," *Frontiers in applied mathematics*, Society for Industrial and Applied Mathematics, Philadelphia, 2002, pp. 139.

[13] Wickert, D.P., Roberts, R.W., and Canfield, R.A., "Least-Squares Continuous Sensitivity Equations for an Infinite Plate with a Hole," Vol. AIAA-2008-1797, 2008.

[14] Étienne, S., and Pelletier, D., "A general approach to sensitivity analysis of fluid–structure interactions," *Journal of Fluids and Structures*, Vol. 21, No. 2, 2005, pp. 169-186.

[15] Etienne, S., Hay, A., Garon, A., "Shape Sensitivity Analysis of Fluid-Structure Interaction Problems," Vol. AIAA 2006-3217, AIAA, 2006.

[16] Etienne, S., Hay, A., Garon, A., "Sensitivity Analysis of Unsteady Fluid-Structure Interaction Problems," Vol. AIAA-2007-332, AIAA, 2007.

[17] Dems, K., and Mroz, Z., "Variational approach by means of adjoint systems to structural optimization and sensitivity analysis. I - Variation of material parameters within fixed domain," *International Journal of Solids and Structures*, Vol. 19, No. 8, 1983, pp. 677-692.

[18] Livne, E., "Future of Airplane Aeroelasticity," *Journal of Aircraft*, Vol. 40, No. 6, 2003, pp. 1066--1092.

[19] Bendiksen, O.O., "Modern developments in computational aeroelasticity," *Journal of Aerospace Engineering*, Vol. 218, 2004, pp. 157.

[20] Hubner, B., Walhorn, E., and Dinkler, D., "A monolithic approach to fluid–structure interaction using space–time finite elements," *Computer Methods in Applied Mechanics and Engineering*, 2004.

[21] Etienne,S. (Ecole Polytechnique de Montreal), "A monolithic formulation for unsteady Fluid-structure Interactions," *Collection of Technical Papers - 44th AIAA Aerospace Sciences Meeting, Collection of Technical Papers - 44th AIAA Aerospace Sciences Meeting*, Vol. 11, 2006, pp. 8301.
[22] Walhorn, E., Kölke, A., Hübner, B., "*Fluid-structure coupling within a monolithic model involving free surface flows*," *Computers and Structures*, Vol. 83, 2005, pp. 2100-2111.
[23] Heys, J.J., Manteuffel, T.A., McCormick, S.F., "First-order system least squares (FOSLS) for coupled fluid-elastic problems," *Journal of Computational Physics*, Vol. 195, No. 2, 2004, pp. 560-575.
[24] Bathe, K., and Zhang, h., "Finite element developments for general fluid flows with structural interactions," *International Journal for Numerical Methods in Engineering*, Vol. 60, 2004, pp. 213-213-232.
[25] Bathe, K., and Shanhong, H.Z., "Finite element analysis of fluid flows fully coupled with structural interactions," *Computer and Structures*, Vol. 72, 1999, pp. 1-1-16.
[26] Kayser-Herold, O., and Matthies, H.G., "A Unified Least-Squares Formulation for Fluid-Structure Interaction Problems," *Computer and Structures*, Vol. 85, 2007, pp. 998-998-1011.
[27] Rasmussen, C.C., Canfield, R.A., and Reddy, J.N., "The Least-Squares Finite Element Method Applied to Fluid-Structure Interaction Problems," AIAA, 2007.
[28] Bochev, P.B., and Gunzburger, M.D., "Finite Element Methods of Least-Squares Type," *SIAM Review*, Vol. 40, No. 4, 1998, pp. 789--837.
[29] Jiang, B., "The least-squares finite element method : theory and applications in computational fluid dynamics and electromagnetics," *Scientific computation*, Springer, Berlin ; New York, 1998, pp. 418.
[30] Yang, S., and Liu, J., "Analysis of Least Squares Finite Element Methods for A Parameter-Dependent First-Order System," *Numerical Functional Analysis and Optimization*, Vol. 19, 1998, pp. 191-213.
[31] Bramble, J.H., Lazarov, R.D., and Pasciak, J.E., " Least-squares methods for linear elasticity based on a discrete minus one inner product." *Comput. Methods Appl. Mech. Engrg.*, Vol. 152, 2001, pp. 520--543.
[32] Proot, M.M.J., "The least-squares spectral element method: theory, implementation and application to incompressible flows," 2003.
[33] Cai, Z., Manteuffel, T., McCormick, S., " *First-order system least squares for the Stokes equations, with application to linear elasticity*," *SIAM Journal of Numerical Analysis*, Vol. 34, No. 5, 1997, pp. 1727--1741.
[34] Pontaza, J.P., "Least-squares finite element formulation for shear-deformable shells," *Computer Methods in Applied Mechanics and Engineering*, Vol. 194, No. 21-24, 2005, pp. 2464.
[35] Kayser-Herold, O., and Matthies, H.G., "Least-Squares FEM Literature Review," Institute of Scientific Computing Technical University Braunschweig, 2005-05, Brunswick, Germany, 2005.
[36] Blair, M., Canfield, R.A., and Roberts, R., "A Joined-Wing Aeroelastic Design with Geometric Non-Linearity," *Journal of Aircraft*, Vol. 42, No. 4, 2005, pp. 832-832–848.
[37] Demasi, L., and Livne, E., "Exploratory Studies of Joined Wing Aeroelasticity," AIAA, 2005.
[38] Hoblit, F.M., "Gust loads on aircraft : concepts and applications," *AIAA education series*, American Institute of Aeronautics and Astronautics, Washington, D.C., 1988, pp. 306.
[39] Reddy, J.N., "An introduction to nonlinear finite element analysis," Oxford University Press, Oxford ; New York, 2004, pp. 463.
[40] Gel'fand, I.M., Fomin, S.V., and Silverman, R.A., "Calculus of variations," Dover Publications, Mineola, N.Y., 2000.
[41] Reddy, J.N., "An introduction to the finite element method," *McGraw-Hill series in mechanical engineering*, McGraw-Hill Higher Education, New York, NY, 2006.
[42] Šolin, P., Segeth, K., and Doležel, I., "Higher-order finite element methods," *Studies in advanced mathematics*, Chapman & Hall/CRC, Boca Raton, FL, 2004.
[43] Szabo, B.A., and Babuška, I., "Finite element analysis," Wiley, New York, 1991.